Supporting Information

On-demand multiplexed vortex beams for terahertz polarization detection based on metasurfaces

Wenhui Xu,‡[a] Hui Li,‡[a] Shouxin Duan,[b] Hang Xu,*[a] Chenglong Zheng,[c] Jie Li,[d] Chunyu Song,[a] Yating Zhang,*[a] Yun Shen,*[b] and Jianquan Yao*[a]

[a] Key Laboratory of Opto-Electronics Information Technology (Tianjin University), Ministry of Education, School of Precision Instruments and Opto-Electronics Engineering, Tianjin University, Tianjin 300072, China. E-mail: yating@tju.edu.cn, jqyao@tju.edu.cn

[b] Department of Physics, School of Physics and Materials Science, Nanchang University, Nanchang 330031, China. E-mail: shenyun@ncu.edu.cn

[c] Information Materials and Device Applications Key Laboratory of Sichuan Provincial Universities, Chengdu University of Information Technology, Chengdu 610225, China.

Part 1. Flowchart of the proposed working mechanism.

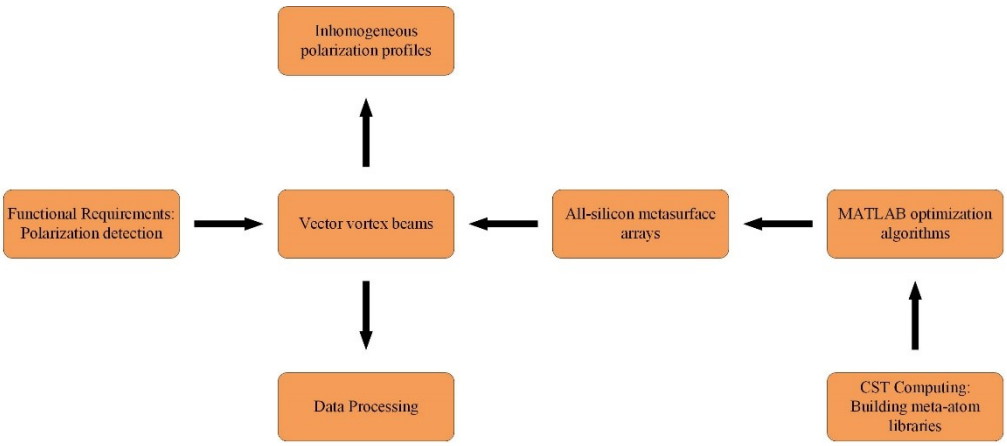

Fig. S1. Flowchart of the proposed design principles.

First, a metasurface-based construction is sought, using a vector vortex beam (VVB) with inhomogeneous polarization distributions as a starting point. It is well known that the commonly used metasurface-based VVBs are generated by embedding helical phases carrying equal amplitude but conjugate topological charges into the LCP and RCP channels, respectively. Therefore, a decoupling mechanism needs to be utilized to break the locking behavior within the orthogonal circularly polarized channels. Next, we calculated and established a parameter library of meta-atoms using the commercial software CST MICROWAVE STUDIO. Subsequently, MATLAB algorithms were coded to further optimize the parameters of the meta-atoms in the established library, and the meta-atoms satisfying the phase requirements were selected. Then, another set of MATLAB algorithms was employed to automatically generate the desired periodicized metasurface array. And, the electric field distribution at the focal plane was reconstructed to discriminate the incident polarization state.

Part 2. Simulation details of all-silicon metasurface with tailored polarization response.

For a single meta-atom: The selection of the basic building blocks with all-silicon construction was performed using the time domain solver of the CST Microwave Studio software. The probe is added at a position approximately twice the working wavelength from the rectangular silicon column, and a plane wave carrying polarization characteristics is incident vertically from the substrate side. It is worth mentioning that the refractive indices of both the rectangular silicon columns and the substrate used in the basic modeling were set to 3.45. The amplitude and phase responses exhibited by all-silicon meta-atoms with periodic boundary conditions in the x- and y-directions are first recorded in the post-processing template of the CST. Subsequently, the structural parameters of the meta-atoms corresponding to the desired phase distribution were extracted using MATLAB.

For the metasurface array: The selected 15 meta-atoms are expanded into an 8×8 parameter matrix satisfying a phase interval of π/4. By loading the file containing the parameter information of the basic building blocks into MATLAB, we are able to flexibly generate a metasurface array that satisfies the phase requirements. Then, the x, y and z directions are set as open boundary conditions. And, the modeling space along the z-direction needs to be slightly larger than the focal length. Finally, the complex amplitude information containing 800×800-pixel points is processed using another MATLAB code when needed.

Part 3. Amplitudes and phase distributions of the meta-atomic library established for different illumination methods.

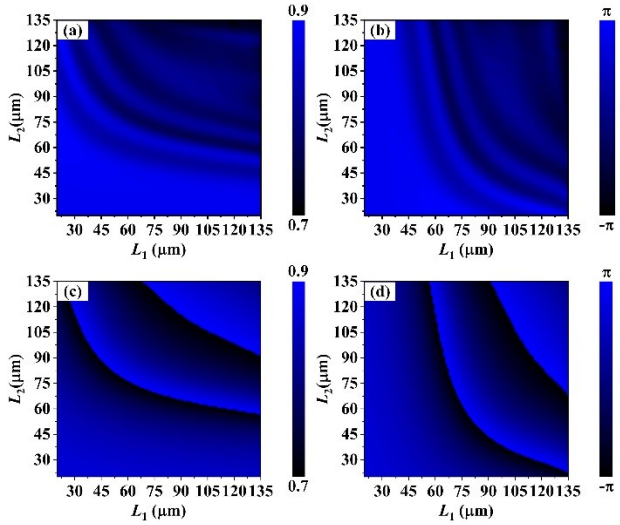

Fig. S2. Transmission amplitudes and phase shifts of the basic building blocks with different geometric sizes, (a, c) under *x*-polarized incidence, and (b, d) under *y*-polarized incidence.

Part 4. Normalized magnetic field intensity at working frequency for meta-atoms with all-silicon configuration.

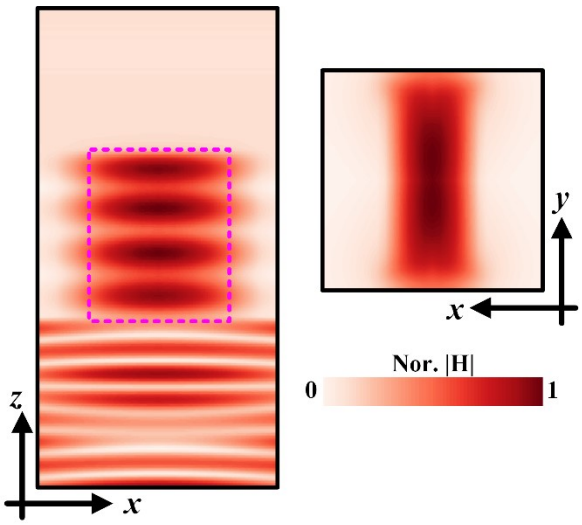

Fig. S3. Normalized magnetic field intensity at working frequency for meta-atoms with all-silicon configuration, implies that the coupling between adjacent building blocks is very weak in meta-arrays that exhibit a quasi-periodic distribution.

Part 5. Amplitude and phase responses of periodized silicon pillars with high aspect ratio under *x*-polarized and *y*-polarized illumination.

As an example, the amplitude and phase response at 0.8 THz of the basic building block with structural parameters L_1=93 μm and L_2=34 μm are shown in Figure S4. With the illumination of THz plane waves with $x(y)$ polarization, the amplitude of the co-polarized component at 0.8 THz is nearly 90%. In addition, the selected meta-atoms have a phase difference of π at orthogonal linearly polarized incidence (p_{xx}=-114.25, p_{yy}=65.86). The oscillations shown in the transmission spectrum can be qualitatively interpreted as Fabry-Perot resonances.

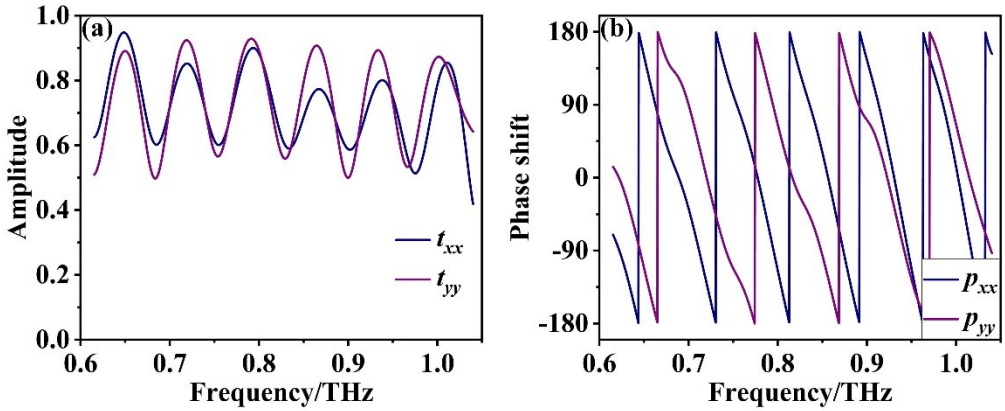

Fig. S4. Stimulated spectra of (a) transmission amplitude and (b) phase shift of the periodized silicon pillars under linearly polarized incidence, respectively.

Part 6. Broadband focusing properties of the proposed metasurface.

In order to quantitatively analyze the focusing performance of the proposed design, we calculated the focusing efficiencies and the corresponding focal lengths in the broadband range from 0.7 THz to 0.9 THz, respectively, as shown in Fig. R1. One can be clearly seen that the focusing efficiencies in the target frequency range are all higher than 51%. Not only that, the focal length increases gradually with increasing frequency due to the chromatic behavior.

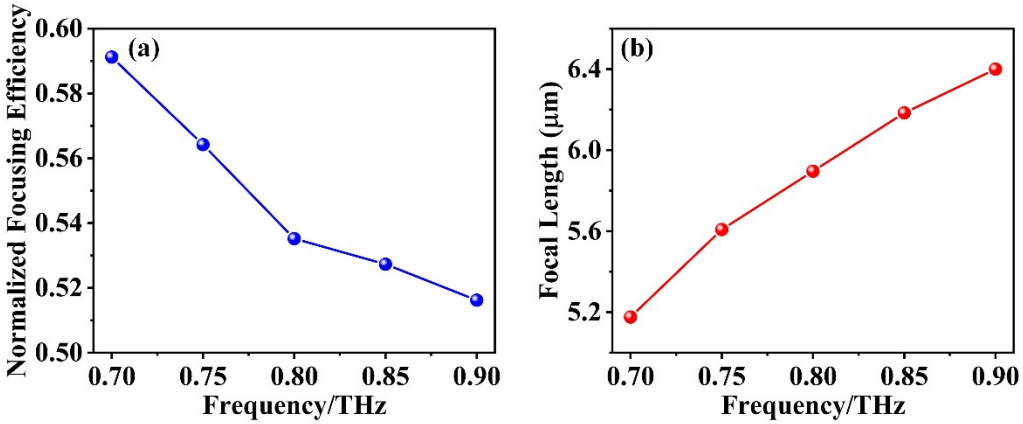

Fig. S5. Broadband focusing properties of the proposed metasurface for evaluation of the incident polarization state. (a) Normalized focusing efficiency, and (b) focal length.

Part 7. Fundamental properties of vector vortex spots generated in the focal plane by the employed polarization multiplexing coding technique.

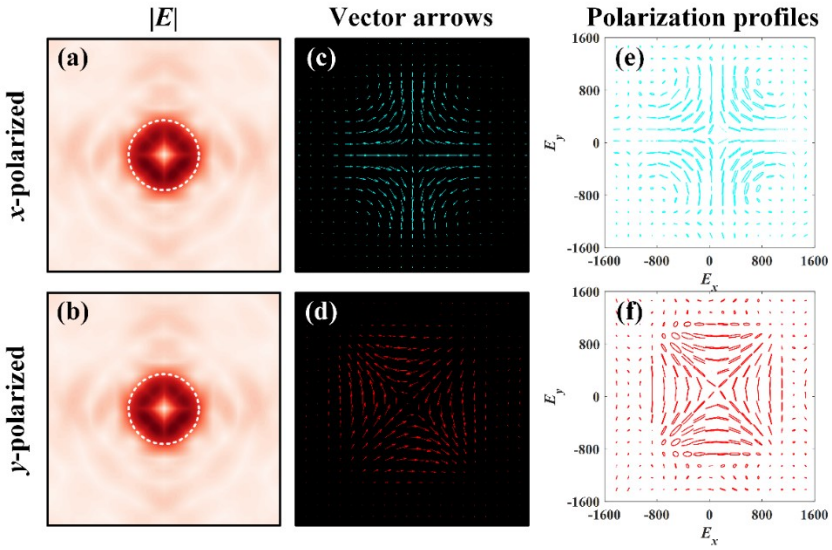

Fig. S6. Fundamental properties of vector vortex spots generated in the focal plane by the employed polarization multiplexing coding technique. The total electric field distribution |E| monitored in the focal plane, including (a) under *x*-polarized incidence and (b) under *y*-polarized incidence. Vector arrows for characterizing inhomogeneous polarization distribution obtained by calculation using MATLAB code (c) under *x*-polarized incidence and (d) under *y*-polarized incidence. The extracted polarization profile with inhomogeneous characteristics corresponds to the focal plane (e) under *x*-polarized incidence and (f) under *y*-polarized incidence.

Part 8. Measurement of the polarization conversion for THz wave.

The employed THz near-field imaging system can only produce a linearly polarized beam in the pump module, while the equipped probe can measure the linearly co- and cross-polarized components. When the fabricated sample is illuminated by circularly polarized THz waves, the circularly polarized components with vectorial characteristics can be obtained by superimposing the complex amplitudes of the four linear polarized components, and then the final polarization state can be judged:

$$\begin{pmatrix} E_{++} & E_{+-} \\ E_{-+} & E_{--} \end{pmatrix} = \frac{1}{2}\begin{pmatrix} E_{xx}+E_{yy}+i\left(E_{xy}+E_{yx}\right) & E_{xx}-E_{yy}-i\left(E_{xy}+E_{yx}\right) \\ E_{xx}-E_{yy}+i\left(E_{xy}+E_{yx}\right) & E_{xx}+E_{yy}-i\left(E_{xy}-E_{yx}\right) \end{pmatrix}, \text{(S1)}$$

where E_{ij} (i, j = +,-) represents the four circular polarization components. In contrast, the cross-polarization component is absent for the E_z-component generated through the spin-orbit coupling effect. Thus, by superimposing the electric field distribution of each linearly polarized component characterized by the Jones matrix, the solution of each transmitted circularly polarized component can be obtained indirectly, which can be usually expressed as follows,

$$E_\sigma = \frac{E_x - i\sigma E_y}{\sqrt{2}}, \text{(S2)}$$

Here, σ = +1 and σ = -1 represent the transmitted LCP and RCP components, respectively.

Part 9. The effect of polarization states varying along a predetermined path on the recorded normalized amplitudes.

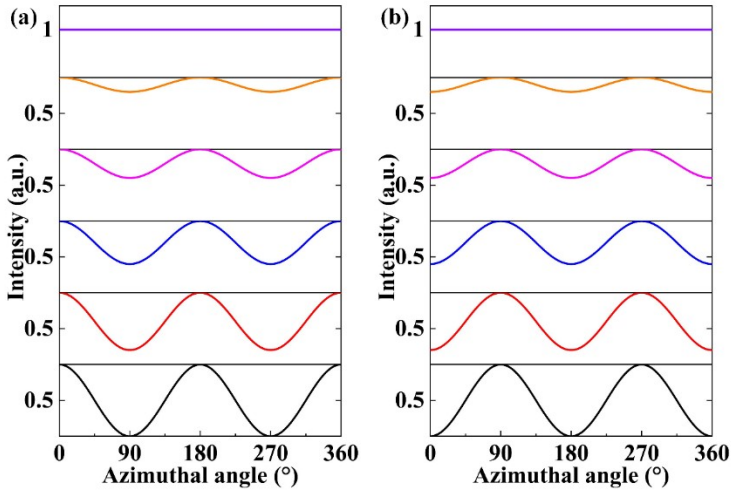

Fig. S7. The effect of polarization states varying along a predetermined path on the recorded normalized amplitudes, (a) when the incident polarization state gradually switches from *x*-polarization to LCP, and (b) when the incident polarization state gradually switches from LCP to *y*-polarization.

Part 10. Theoretical derivation of the longitudinal polarization component produced by a vortex beam with tightly focusing behavior.

The focused electric field of a vortex beam with topological charge l generated on the metasurface under illumination by circularly polarized waves can be expressed as,

$$\begin{aligned} E(r,\varphi,z) &= \begin{bmatrix} E_x \\ E_y \\ E_z \end{bmatrix} = -\frac{ikf}{2\pi}\int_0^{\theta_m}\int_0^{2\pi} A(\theta)\exp(il\phi)\sin\theta\sqrt{\cos\theta} \\ &\times\exp\left[ik\left(z\cos\theta + r\sin\theta\cos(\phi-\varphi)\right)\right] \\ &\times\begin{bmatrix} \left(\cos^2\phi\cos\theta+\sin^2\phi\right) \pm i\cos\phi\sin\phi\left(\cos\phi-1\right) \\ \cos\phi\sin\phi\left(\cos\phi-1\right)\pm i\left(\cos^2\phi+\sin^2\phi\cos\theta\right) \\ \sin\theta\exp(\pm i\phi) \end{bmatrix} d\phi d\theta, \end{aligned} \quad \text{(S3)}$$

Where (r, φ, z) represent the cylindrical coordinate systems, φ denotes the azimuthal angle of the incident THz waves, θ_m=arcsin(NA) indicate the maximum aperture angle of the device, f is the focal length, and k represents the wave vector. After coordinate transformation, the pupil apodization $A(\theta)$ can be expressed as,

$$A(\theta) = \exp\left(-f^2\sin^2\theta / w^2\right), \quad \text{(S4)}$$

As a consequence, the E_z-component of the monitored electric field distribution at the focal plane can be described as,

$$\begin{aligned} E_{\pm,z}(r,\varphi,z) &= -ikf\exp\left[i(l\pm1)\phi\right]\int_0^{\theta_m} A(\theta)\sin^2\theta \\ &\sqrt{\cos\theta}e^{ikz\cos\theta}i^{l\pm1}J_{l\pm1}(kr\sin\theta)d\theta, \end{aligned} \quad \text{(S5)}$$

The tightly focusing behavior of the vortex beam can invoke the conversion of the SAM of the photon to the OAM. The SAM of the incident circularly polarized THz wave can be partially converted to the OAM of the longitudinally polarized electric field (E_z), resulting in a vortex beam with a doughnut-shaped intensity distribution. The design principle of this metasurface is the multiplexing of two orthogonal circularly polarized channels, allowing independent manipulation of the phase profile within each channel. Therefore, for the incident LCP beam, the transmitted transverse polarization distribution can be decomposed into LCP and RCP components, carrying topological charges defined as l_1 and l_2, respectively. Then, the transmitted E_z-component of the electric field can be expressed as,

$$\begin{aligned} E_{LCP,z} &= B\exp\left[i(l_1-1)\phi\right]\int_0^{\theta_m} A(\theta)Ci^{l_1-1}J_{l_1-1}(kr\sin\theta)d\theta \\ &+B\exp\left[i(l_2+1)\phi\right]\int_0^{\theta_m} A(\theta)Ci^{l_2+1}J_{l_2+1}(kr\sin\theta)d\theta, \end{aligned} \quad \text{(S6)}$$

Here,

$$\begin{cases} B = -ikf \\ C = \sin^2\left(\cos\theta\right)^{\frac{1}{2}} \exp\left(ikz\cos\theta\right) \end{cases}, \quad \text{(S7)}$$

Where $J_s\left(kr\sin\theta\right)$ denotes the *s*-order Bessel function of the first type. Obviously, the resulting longitudinal polarization component contains both vortex fields with topological charges of l_1-1 and l_2+1, respectively. If the incident wave is sw

itched to RCP mode under constant conditions, the resulting longitudinal polarization component E_z can be described as,

$$\begin{aligned} E_{RCP,z} &= B\exp\left[i\left(l_3-1\right)\phi\right]\int_0^{\theta_m} A\left(\theta\right)Ci^{l_3-1}J_{l_3-1}\left(kr\sin\theta\right)d\theta \\ &+B\exp\left[i\left(l_1+1\right)\phi\right]\int_0^{\theta_m} A\left(\theta\right)Ci^{l_1+1}J_{l_1+1}\left(kr\sin\theta\right)d\theta \end{aligned} \quad \text{(S8)}$$

It can be clearly seen that the topological charges carried by the longitudinally polarized vortices produced in the RCP illumination mode are l_3-1 and l_1+1, respectively. Therefore, by reasonably modifying the topological charges l_1, l_2 and l_3, the distribution of the generated longitudinal polarization field can be flexibly tailored.